

Exploring α decay properties in the superheavy region through the double-folding formalism and Skyrme interactions

O. N. Ghodsi  and M. M. Amiri **Department of Physics, Faculty of Science, University of Mazandaran, P.O. Box 47415-416, Babolsar, Iran*

(Received 23 June 2021; accepted 6 October 2021; published 25 October 2021)

In this study, α decay properties of yet unknown nuclei are investigated through the systematic behavior of the parameters of α -nucleus double-folding (DF) potentials. To calculate DF potentials, the density distributions of the protons and neutrons are being employed by use of the self-consistent Hartree-Fock-Bogoliubov (HFB) calculations based on the SLy4 Skyrme interaction widely used for the α -emitter systems and the superheavy region. In addition, a new set of effective Skyrme force parameters is presented so that more precise estimations, labeled OMGA, are optimized to describe the ground-state properties of superheavy nuclei with $82 \leq Z \leq 120$. Consequently, a good mass fit and half-lives are thus obtained by the optimized Skyrme force with more consistency with experimental data.

DOI: [10.1103/PhysRevC.104.044618](https://doi.org/10.1103/PhysRevC.104.044618)

I. INTRODUCTION

Over the past decade, analyses of the α decay chains have attracted much interest for investigating the nuclear properties of heavy and superheavy nuclei (SHN), which acts as an effective probe for the nuclear structure [1–8]. Exploring concepts of the nuclear structure of new elements are well-known theoretical and experimental research fields in modern nuclear physics.

α decay is indispensable to identify new elements through the observation of α decay from unknown nuclei because the dominant decay mode for SHN is α decay. On the other hand, investigations of α decay chains can provide reliable information on nuclear structure such as ground-state energies, Q values, half-lives, and nuclear spins and parities of new elements in the superheavy region [9–15].

To date, many SHN have been synthesized by cold and hot fusion reactions within developed facilities and technologies [16–20]. Experimentally, synthesis of the $Z = 118$ element is reported by using ^{48}Ca -induced complete fusion reactions in the neutron-evaporation channels [21]. The unknown nucleus $^{296}118$ is a nucleus on which various studies have been performed. Sobiczewski determined the Q_α of the nucleus $^{296}118$ between 10.93 and 13.33 MeV by employing various mass models [3], which led to α decay half-lives of $^{296}118$ ranging over more than five orders of magnitude between 1.4 μs and 0.21 s by using phenomenological formulas [22]. Such a considerable uncertainty originates from a relatively large range of the determined Q_α through the different mass models.

The developed mass models introduced by Wang and Liu (WS3^+) [23], Wang *et al.* ($\text{WS4} + \text{RBF}$) [24], and Muntian *et al.* (HN) [25] constrain the range of Q_α for $^{296}118$. The estimated Q_α for $^{296}118$ are 11.62, 11.73, and 12.06 MeV, and

their corresponding α decay half-lives are 4.8, 2.7, and 0.5 ms for WS3^+ , $\text{WS4} + \text{RBF}$, and HN, respectively. Very recently, the half-life for $^{296}118$ of 14–285 μs by using $Q_\alpha = 12.4$ MeV was reported by Ismail *et al.* [26]. Although the mass models validated known nuclei, the determination of their corresponding anticipations would be challenging for the next unknown nuclei.

Likewise, a delicate procedure demonstrated by considering the smooth and systematic behavior of α decay parameters used for normalizing nucleon-nucleon (NN) interaction in the double-folding (DF) framework very recently predicted the α decay properties of the unknown nucleus $^{296}118$ [1,27]. The Q_α and α decay half-life 11.655 ± 0.095 MeV and 0.825 ms were estimated with an uncertainty of about a factor of four.

Additionally, a good understanding of nuclear structures has been achieved by a wide variety of Skyrme forces associated with the various nuclear-matter properties [28–31]. This approach has been proven to be successful in describing the properties of finite nuclei. Furthermore, the HFB in the coordinate basis associated with the effective Skyrme force has been developed to account for examining the ground-state properties of nuclei [32–35]. Such investigations have been pursued, especially in the nuclear chart regions where the experiments are being performed. Hence the nuclear properties such as binding energies, root-mean-square (rms) radii of the proton and neutron, and density distributions of the nuclei that are being achieved by Skyrme-HFB would be as reputable as possible.

On the other hand, the density distributions play a substantial role in calculating the interaction potential. Inspired by experimental α -scattering data, the capability of DF formalism to calculate α -core potentials came up with the idea that its association with more realistic density distributions suggesting by characterized Skyrme-HFB would be beneficial for analyzing nuclear properties of known and unknown nuclei. However, it would be valuable to give some systematic

*morteza.moghaddari@stu.umz.ac.ir

investigation and comparison of Q values and half-lives of SHN with available mass models. To this aim, considering the gentle and systematic behavior of α decay parameters using DF potentials and the appropriate density distributions of SHN as suggested by the HFB model based on Skyrme forces, we estimate the nuclear properties of $^{296}118$ and the closest unknown SHN.

This paper is organized as follows: The formalism of the potential and half-life calculations are given in Sec. II, and our results and discussion are given in Sec. III. This paper ends with the main results and conclusions presented in Sec. IV.

II. THEORETICAL FRAMEWORK

A. Double-folding formalism and the α decay half-life

The determination of interaction potential is one the predominant factors on the theoretical studies. The effective α -core potential $V(R)$ is given by

$$V(R) = V_C(R) + V_N(R) + \frac{L(L+1)\hbar^2}{2\mu R^2}, \quad (1)$$

where $V_C(R)$ and $V_N(R)$ are the Coulomb and nuclear parts of the total potential, respectively. Also, R denotes the vector joining the center of masses of the two nuclei. In this study, we investigate the α decay of even-even nuclei for which the transferred angular momentum L for these decay processes is zero. The nuclear part is obtained by the double-folding model within folding the densities of the alpha and the daughter nuclei with the effective M3Y interaction,

$$V_N(R) = \lambda V_F(R) \\ = \lambda \iint \rho_1(\mathbf{r}_1) V_{\text{eff}}(\mathbf{s}) \rho_2(\mathbf{r}_2) d^3\mathbf{r}_1 d^3\mathbf{r}_2, \quad (2)$$

where $\mathbf{s} = \mathbf{R} + \mathbf{r}_1 - \mathbf{r}_2$ corresponds to the distance between two specified interacting points of the interacting nuclei, whose radius vectors are \mathbf{r}_1 and \mathbf{r}_2 , respectively. $V_{\text{eff}}(\mathbf{s})$ is an effective nucleon-nucleon interaction [36,37]. The energy-dependent M3Y Reid- NN forces with the zero-range approximation used in our calculations have following explicit forms [38]:

$$V_{\text{eff}}(\mathbf{s}) = 7999 \frac{\exp(-4s)}{4s} - 2134 \frac{\exp(-2.5s)}{2.5s} + J_{00}\delta(\mathbf{s}), \\ J_{00} = -276(1 - 0.005E/A). \quad (3)$$

In addition, the density distributions of the alpha and daughter nucleus in density-dependent formalisms such as the DF model have great importance. Hence it would be possible that the choice of more realistic density distributions would result in better predictions. In Eq. (2), ρ_1 is taken for the density distribution function of the spherical α particle in its Gaussian form used in this study [39]. Furthermore, ρ_2 is the density of the daughter nucleus that is determined by HFB calculations based on the set of Skyrme SLy4 parametrization [30,40] as a result of its capability for well reproducing the α decay energies and density distributions of heavy and super-heavy nuclei, in this study [33,41]. Also, an optimized set of Skyrme parametrization dedicated to the α -emitter systems in

the superheavy region for promoting our calculations will be introduced in the following.

Although the semimicroscopic DF potentials based on the effective Michigan-3-Yukawa (M3Y) NN interaction can well reproduce most of the scattering data, they fail to describe many reactions that are strongly affected by the characteristics of the potential below the barrier in the internal region [42]. This deficiency can be due to the nonconsideration of the repulsive core in the DF model [36,43]. To compensate this deficiency, the Bohr-Sommerfeld (BS) quantization condition has been used to renormalize the strength of effective NN interactions that support alpha clusterization on the surface regions [44–47]. To achieve this, the λ parameter in Eq. (2) changes the folded potential strength that is known as the strength parameter. It can be determined by using the BS quantization condition [48–50]:

$$\int_{R_1}^{R_2} \sqrt{\frac{2\mu}{\hbar^2} |V(R) - Q|} dR = (2n+1) \frac{\pi}{2} = (G-L+1) \frac{\pi}{2}, \quad (4)$$

where R_2, R_3 are classical turning points and are obtained by $V(R) = Q$ (the α decay energy), and for $0^+ \rightarrow 0^+$ s -wave decay the inner turning point is at $R_1 = 0$. In the BS quantization condition concept, a one-dimensional effective normalized potential reproducing the α decay energy in the total system is being obtained. Hence the BS condition normalizes the potentials oriented with respect to the deformations by considering the constant Wildermuth condition; the same effective potentials with a fair approximation would be expected. Therefore, effective λ parameters are considered for the nuclei with large deformations, which can almost reproduce the α decay energy in all oriented angles.

The global quantum number G of a cluster state can be obtained by the Wildermuth condition [51]:

$$G = 2N + L = \sum_{i=1}^4 g_i, \quad (5)$$

where N is the number of nodes of the α -core wave function; L is the relative angular momentum of the cluster motion, and g_i is the oscillator quantum number of a cluster nucleon. For the α decay, we can take G as 18 for $N < 82$, 20 for $82 < N \leq 126$, and 22 for $N > 126$.

Finally, the half-life of the α decay is $T_{1/2} = \hbar \ln 2 / \Gamma_\alpha$. In this relation, Γ_α is the α decay width of the cluster state within the Gurvitz and Kälbermann method, determined as [52]

$$\Gamma_\alpha = F P_\alpha \frac{\hbar^2}{4\mu} \exp\left(-2 \int_{R_2}^{R_3} k(R) dR\right), \quad (6)$$

where F is a normalization factor that can be defined as

$$F \int_{R_1}^{R_2} \frac{dR}{2k(R)} = 1. \quad (7)$$

$k(R) = \{2\mu/\hbar^2[V(R) - Q]\}^{1/2}$ is the wave number. Also, P_α and μ are the alpha-formation probability and reduced mass, respectively.

B. Cluster formation model

Recently, the competition between α decay and spontaneous fission is analyzed in detail, and the decay modes are predicted for the unknown nuclei, and they reported that the our desired SHN have an α decay mode [53]. Also, due to the fact that most SHN are α emitters, the α decay process is being considered in the preformed cluster model (PCM) in this study. It is assumed that the α cluster forms first in the surface region of the parent nucleus, with the preformation probability given by the α -preformation factor P_α and then the tunneling process from the Coulomb barrier is going on.

Within the cluster-formation model (CFM), the total clusterization state Ψ of parent nuclei is assumed as a linear combination of all its N possible clusterization states [54]. For each preformation, there is a different wave function and a different Hamiltonian. Therefore, a clusterization state represented by a wave function is assumed for each preformation or clusterization. If the parent nucleus has N different clusterization states with total energy E , the Hamiltonian H_i belongs to the i th clusterization defined with an i th wave function, therefore

$$H_i \Psi_i = E \Psi_i, \quad i = 1, 2, \dots, N. \quad (8)$$

Therefore, this nucleus is described by a total time-independent wave function that is a linear combination of these clusterization orthonormalized wave functions:

$$\Psi = \sum_{i=1}^N a_i \Psi_i, \quad (9)$$

where a_i are the amplitudes for the clusterization states of the complete set and within the orthogonality condition,

$$\sum_i^N |a_i|^2 = 1. \quad (10)$$

Each cluster has a specific formation energy E_{fi} with

$$E_{fi} = |a_i|^2 E. \quad (11)$$

The probability of the alpha clusterization state P_α is equivalent to a_α^2 . It can be calculated as

$$P_\alpha = |a_\alpha|^2 = \frac{E_{f\alpha}}{E}, \quad (12)$$

where a_α and $E_{f\alpha}$ denote the coefficient of the α clusterization and the formation energy of an α cluster, respectively. E is composed of $E_{f\alpha}$ and the interaction energy between the α cluster and the daughter nuclei. Detailed illustrations are provided in Ref. [54]. In the framework of the CFM, the α cluster formation energy $E_{f\alpha}$ and total energy E of a considered system can be expressed as

$$E_{f\alpha} = 3B(A, Z) + B(A - 4, Z - 2) - 2B(A - 1, Z - 1) - 2B(A - 1, Z), \quad (13)$$

$$E = B(A, Z) - B(A - 4, Z - 2), \quad (14)$$

where $B(A, Z)$ is the binding energy of the nucleus with mass number A and proton number Z . The energies defined in

Eqs. (13) and (14) belong to even-even nuclei, and for an odd atomic number or odd neutron number, the formation energies can be found in Refs. [55,56]. Moreover, the formation probability of each cluster state calculated by the CFM can well reproduce a more realistic formation probability, which follows the calculation of Varga *et al.* [57,58].

III. RESULTS AND DISCUSSIONS

Microscopic HFB and relativistic-mean-field theories are useful models which have been used to calculate ground-state properties of nuclei [59–61]. On the other hand, the α decay process is also a low-energy phenomenon, and it cannot actually cause an impressive variation in the ground-state properties of an α emitter [54,62]. Consequently, in this study, the same Skyrme forces constructed to be effective forces for nuclear mean-field calculations are employed to simultaneously reproduce the ground-state properties of parent and daughter nuclei on the α decay process. Due to the unstable structures of SHN, the choice of appropriate mean fields that are describing the nuclear properties of SHN is increasingly noticeable. It is desirable to represent such appropriate mean fields of effective density-dependent forces as much as possible. The Skyrme interaction, originally constructed for finite nuclei and nuclear matter at saturation density, is a low-momentum expansion of the effective two-body NN interaction in momentum space. This approach is based on the parametrization of such forces fit to the ground-state properties of stable nuclei, fission barriers, and symmetric and asymmetric nuclear matter (ANM).

It is valuable to keep in mind that various Skyrme parametrizations were often constructed to emphasize a particular selection of data on finite nuclei. In the present study, the mean fields that are dedicated to the α -emitter systems in the superheavy region are considered. To this end, the Skyrme SLy4 parametrization that has been almost used for the heavy and superheavy regions is being employed associated with a new Skyrme interaction. In this way, this optimized Skyrme interaction parameters, named OMGA, are obtained by self-consistent Hartree-Fock calculations that set comprehensively to the experimental binding energies for the region with $82 \leq Z \leq 120$. It is noticeable that these two forces have the same underlying literature.

The important point about the Skyrme interaction is that it has a phenomenological structure in which some correlation effects are included through its parameters. The energy per nucleon of an infinite ANM with a proton fraction $\eta = Z/A$ in terms of the Skyrme energy density function is written as

$$E_A = \frac{3\hbar^2}{10m} k_F^2 H_{5/3} + \frac{t_0}{4} \rho \left[(x_0 + 2) - \left(x_0 + \frac{1}{2} \right) H_2 \right] + \frac{t_3 \rho^{\sigma+1}}{24} \left[(x_3 + 2) - \left(x_3 + \frac{1}{3} \right) H_2 \right] + \frac{3k_F^2}{40} \left\{ (2t_1 + 2t_2 + t_1 x_1 + t_2 x_2) \rho H_{5/3} + \left(\frac{t_2}{2} - \frac{t_1}{2} + t_2 x_2 - t_1 x_1 \right) \rho H_{8/3} \right\}, \quad (15)$$

where $k_F = (3\pi^2\rho/2)^{1/3}$ and $H_n(\eta) = 2^{n-1}[\eta^n + (1-\eta)^n]$. The parameters $x_0 - x_3$, $t_0 - t_3$, W_0 , and σ are obtained by fitting different properties of nuclei, m is the nucleon mass, and ρ is the nuclear density. One should note that there are several other sets of parameters which parametrize the density dependence of the Skyrme functional in ways different from those considered here, which are not included in the present study. Equation (15) leads to an in-medium effective nucleon mass m^* in ANM of

$$m^* = m \left\{ H_{5/3} + \frac{m}{4\hbar^2} \rho [aH_{5/3} + bH_{8/3}] \right\}^{-1}, \quad (16)$$

with $a = t_1(x_1 + 2) + t_2(x_2 + 2)$ and $b = 1/2[t_2(2x_2 + 1) - t_1(2x_1 + 1)]$. The symmetry energy E_{sym} indicating differences between energies of the symmetric and asymmetric states is defined by expanding Eq. (15) as a function of η and ρ that measures the isospin dependence of the NN interaction as

$$E_{\text{sym}}(\rho) = \frac{1}{8} \left. \frac{\partial^2 E_A(\rho, \eta)}{\partial \eta^2} \right|_{\eta=1/2} = \frac{\hbar^2 k_F^2}{6m} - \frac{t_0}{4} \left(x_0 + \frac{1}{2} \right) \rho - \frac{t_3}{24} \left(x_3 + \frac{1}{2} \right) \rho^{\sigma+1} + \frac{k_F^2}{24} \{ (4t_2 - 3t_1x_1 + 5t_2x_2) \rho \}. \quad (17)$$

The Skyrme interaction, originally constructed for finite nuclei and nuclear matter at saturation density ρ_0 , and the determination of the saturation density is associated with the nuclear matter properties of ANM. Also, the pressure is defined as $P = \rho^2 \frac{\partial(E_A)}{\partial \rho}$, and the volume incompressibility K of ANM at saturation density is calculated as the derivative of pressure with respect to the number density ρ :

$$K = 9 \frac{\partial P}{\rho} = 9\rho^2 \left(\frac{\partial^2 E_A}{\partial \rho^2} \right). \quad (18)$$

In the Skyrme-HFB formalism, the evaluation of the expectation energy leads to an expression that is a functional of the local densities. The coordinate-space solution of the Skyrme-HFB and contact-pairing force equations for calculating the local densities is discussed in Ref. [63], which is used in this study.

In addition, the nucleon density distribution has impressive importance in assessing nuclear properties impacting the interaction potential [64–68]. Hence we use the nucleon density distributions suggesting by the SLy4 Skyrme interaction. On the other hand, the OMGA Skyrme force is being parametrized for achieving more precise anticipations about the experimental binding energies in the superheavy region. For better recognizing, the Skyrme parameters of the SLy4 and OMGA are listed in Table I.

Furthermore, the inherent nuclear matter properties of each SLy4 and OMGA forces are illustrated in Table II. By considering the equilibrium densities in Table II, one might hope that OMGA is also stable against collapse as the SLy4 force due to its capability to satisfy the nuclear matter properties at saturation density. Also, the higher K_0 of the OMGA estimates more dense structures for the SHN, which would impact the α

TABLE I. Parameters of the SLy4 and OMGA Skyrme interactions.

Parameters	SLy4	OMGA
t_0 (MeV fm ³)	−2488.91	−1844.98
t_1 (MeV fm ⁵)	486.820	473.830
t_2 (MeV fm ⁵)	−546.390	1006.860
t_3 (MeV fm ^{3+σ)}	13777.00	9688.45
x_0	0.8340	0.4035
x_1	−0.3440	−2.8950
x_2	−1.0000	−1.3135
x_3	1.3540	0.9550
a	0.166667	0.258200
W_0 (MeV fm ⁵)	123.000	165.000

decay properties [62]. Furthermore, the obtained incompressibility K_0 within the OMGA force is in agreement with the values reported in Ref. [69].

For comparison, the capabilities of SLy4 and OMGA Skyrme interactions for reproducing experimental binding energies are considered. Hence the calculated binding energies within these Skyrme interactions for the desired even-even nuclei with $82 \leq Z \leq 120$ are being compared with their corresponding experimental data. To have a better insight into their deviations from experimental data, the ratios $B^{\text{Cal}}/B^{\text{Expt}}$ for the SLy4 and OMGA are illustrated in Fig. 1(a). Also, the standard deviations of the present calculations, 25.783 and 4.042, respectively, are obtained for SLy4 and OMGA within $\sigma = [\frac{1}{N} \sum_{i=1}^{N=32} (B_i^{\text{Cal}} - B_i^{\text{Expt}})^2]^{1/2}$. As shown in this figure and by the obtained standard deviations, the calculated binding energies within the OMGA force are more consistent with the experimental data than the SLy4 force.

As additional information, the rms radius is important to estimate nuclear properties, indicating the capability of forces to describe nuclear properties. Owing to the fact that the experimental rms charge radii have not been reported yet for most SHN, the semi-empirical relation $R_{\text{Ch}} = (r_0 + r_1 A^{-2/3} + r_2 A^{-4/3}) A^{1/3}$ is also employed and is quoted as $R_{\text{Ch}}^{\text{Expt}}$ in the following, and the parameters are $r_0 = 0.9071(13)$ fm, $r_1 = 1.105(25)$ fm, and $r_2 = -0.548(34)$ fm. This relation is obtained by fitting to the experimental data of the ground-state rms charge radii for a wide range of the nuclei [70]. Consequently, the rms charge radii originating from SLy4 and OMGA are concerned and the ratios $R_{\text{Ch}}^{\text{Cal}}/R_{\text{Ch}}^{\text{Expt}}$ for SLy4 and OMGA are illustrated in Fig. 1(b). To have a better insight into their deviations from experimental data, the standard deviation

TABLE II. Nuclear matter properties of the SLy4 and OMGA Skyrme interactions.

	SLy4	OMGA
ρ_0 (fm ^{−3})	0.160	0.156
E_0 (MeV)	−15.970	−15.800
K_0 (MeV)	229.910	246.803
S_0 (MeV)	31.986	37.766
m^*/m	0.694	0.646

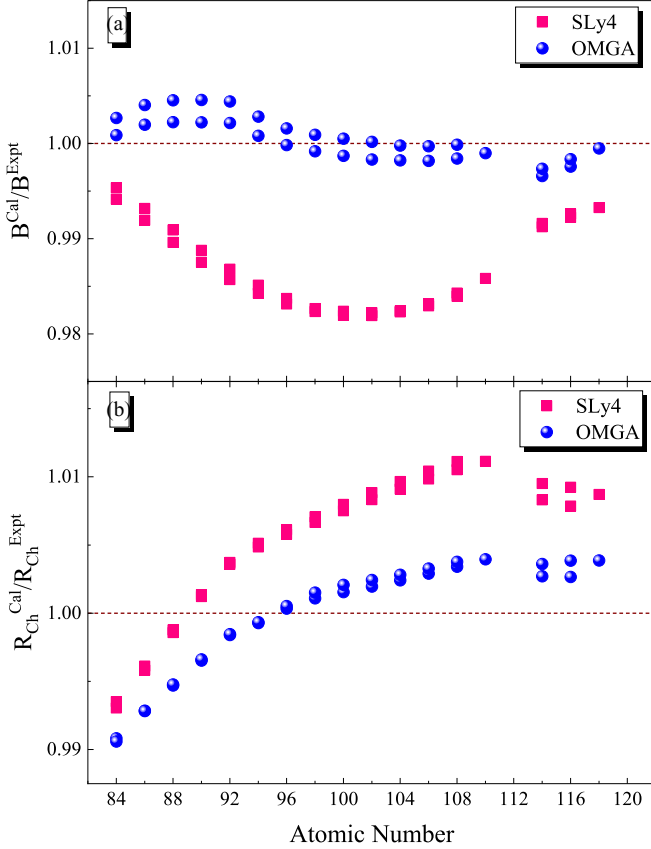


FIG. 1. (a) The deviations of calculated binding energies obtained by SLy4 and OMGA from their corresponding experimental values. (b) The deviations of calculated rms charge radii obtained by SLy4 and OMGA from their corresponding semi-empirical values.

tions 0.044 and 0.023 corresponding to the SLy4 and OMGA forces are obtained by $\sigma = [\frac{1}{N} \sum_{i=1}^{N=32} (R_{Ch(i)}^{Cal} - R_{Ch(i)}^{Expt})^2]^{1/2}$. Furthermore, from the analysis of this yield [71], the rms nuclear charge radii was expressed as

$$\sqrt{R_{Ch}} = [X_1 - X_2 \log_{10}(T_{1/2})]/\xi_1 \xi_2 + X_3 \xi_1 Q_\alpha^{-1/2}, \quad (19)$$

where the parameters X_1 , X_2 , and X_3 , for $Z \geq 82$ and $N \geq 126$ are $-15.8767(942)$, $0.6213(30)$, and $0.7975(26)$, respectively. Also, $\xi_1 = (Z_1 Z_2 e^2)^{1/2}$ and $\xi_2 = \sqrt{2\mu}/\hbar$ are considered. To estimate the rms nuclear charge radii by the mentioned relation, the adopted experimental values of $T_{1/2}$ and Q_α are listed in Table III. For further comparison, the standard deviations 0.409 and 0.377 are obtained for the estimated rms charge radii with SLy4 and OMGA forces from their corresponding values calculated by the above relation.

To have a further evaluation, the rms nuclear charge radii originating from SLy4 and OMGA forces are compared with their corresponded values explored by the relativistic continuum Hartree-Bogoliubov theory [72]. The estimated standard deviations of the rms charge radii are 0.042 and 0.032 for SLy4 and OMGA forces, respectively. Overall, one can expect that the Skyrme OMGA force would be more elegant in precise investigations of the superheavy region.

TABLE III. Nuclear properties and logarithms of half-lives for desired α decay chains. The half-lives are being calculated in units of seconds.

Parent	Q_α [MeV]	$T_{1/2}^{Expt}$	P_α^{CFM}	$T_{1/2}^{SLy4}$	$T_{1/2}^{OMGA}$
²⁹² ₁₁₆ Lv	10.7741	-1.7447	0.19	-2.0772	-2.1948
²⁸⁸ ₁₁₄ Fl	10.0721	-0.0969	0.18	-0.8047	-0.9172
²⁹⁴ ₁₁₈ Og	11.8111	-2.7447	0.17	-3.9188	-4.0385
²⁹⁰ ₁₁₆ Lv	10.9921	-1.8239	0.18	-2.6005	-2.6975
²⁸⁶ ₁₁₄ Fl	10.3721	-0.3979	0.18	-1.6194	-1.7163
²⁷⁰ ₁₁₀ Ds	11.1169	-4.0000	0.18	-4.6184	-4.5432
²⁶⁶ ₁₀₈ Hs	10.3456	-2.6383	0.16	-3.3009	-3.2256
²⁶² ₁₀₆ Sg	9.5997	-1.5036	0.16	-1.9360	-1.8691
²⁵⁸ ₁₀₄ Rf	9.1927	0.4164	0.17	-1.4191	-1.3800
²⁵⁴ ₁₀₂ No	8.2263	1.7533	0.14	0.9893	1.0674
²⁵⁰ ₁₀₀ Fm	7.5565	3.3010	0.15	2.6292	2.7201
²⁴⁶ ₉₈ Cf	6.8616	5.1097	0.15	4.6577	4.7654
²⁴² ₉₆ Cm	6.2156	7.1482	0.12	6.8987	7.0112
²³⁸ ₉₄ Pu	5.5932	9.4418	0.14	9.2325	9.3468
²³⁴ ₉₂ U	4.8577	12.8897	0.15	12.8480	12.9751
²³⁰ ₉₀ Th	4.7698	12.3762	0.19	12.2826	12.4274
²²⁶ ₈₈ Ra	4.8706	10.7029	0.18	10.5374	10.6930
²²² ₈₆ Rn	5.5903	5.5186	0.22	5.1785	5.3921
²¹⁸ ₈₄ Po	6.1147	2.2695	0.20	1.7832	1.9665
²⁶⁴ ₁₀₈ Hs	10.5906	-2.7959	0.18	-3.8445	-3.8893
²⁶⁰ ₁₀₆ Sg	9.9005	-2.1427	0.18	-2.6826	-2.7729
²⁵⁶ ₁₀₄ Rf	8.9256	0.3190	0.15	-0.4793	-0.5576
²⁵² ₁₀₂ No	8.5485	0.5633	0.16	-0.0155	-0.1013
²⁴⁸ ₁₀₀ Fm	7.9944	1.5601	0.16	1.1205	1.0327
²⁴⁴ ₉₈ Cf	7.3288	3.0660	0.15	2.8783	2.7571
²⁴⁰ ₉₆ Cm	6.3978	6.3701	0.14	6.0978	5.9958
²³⁶ ₉₄ Pu	5.8670	7.9552	0.16	7.8276	7.7026
²³² ₉₂ U	5.4136	9.3370	0.17	9.3843	9.2608
²²⁸ ₉₀ Th	5.5200	7.7798	0.18	7.7695	7.6313
²²⁴ ₈₈ Ra	5.7888	5.4964	0.18	5.3923	5.2564
²²⁰ ₈₆ Rn	6.4046	1.7451	0.22	1.5822	1.3860
²¹⁶ ₈₄ Po	6.9063	-0.8386	0.21	-1.2106	-1.4065

According to the obtained results, one can expect that the nucleon density distributions calculated by the OMGA force would be reliable for calculating interaction potentials within the DF model. Hence the density distributions obtained from OMGA associated with their corresponding values obtained from SLy4 are being used in this study.

Since we intend to investigate the α decay properties of yet-unknown SHN through the systematic behavior of parameters of α -nucleus DF potentials, a more realistic DF potential based on the M3Y interactions would be beneficial. Due to the fact that the zero-range approximation associated with the central forces of the M3Y interactions cannot satisfy the saturation-density properties [38], some modifications have been applied to the DF model [73,74]. The concept of overlapping densities of participating nuclei is predominantly

associated with the interaction potentials at the partial and full overlap density regions of a dinuclear system [43,73–75]. Therefore, the interior region of interaction potential that two nuclei have a significant overlap can be affected by the nature of NN interactions.

In our previous work [43], we discussed the repulsive NN interactions arising from the Pauli exclusion principle and their effects on the DF formalism, which is not well-embedded in the DF formalism. Such effects were sought as a modification term by investigating the contribution of the kinetic-energy variation at the overlapping regions between the alpha and daughter nuclei densities. For estimating the kinetic-energy well illustrated in density-functional theory (DFT) [76,77], the self-consistent Hartree-Fock calculations are being performed comprising SLy4 and OMGA Skyrme interactions. The variation of the kinetic energy of the density overlap of two colliding nuclei based on the DFT is obtained by

$$\begin{aligned} \Delta K(R) = & \frac{\hbar^2}{2m} \iint \{ \tau[\rho_{1p}(\mathbf{r}) + \rho_{2p}(\mathbf{r} - \mathbf{R}), \rho_{1n}(\mathbf{r}) \\ & + \rho_{2n}(\mathbf{r} - \mathbf{R})] - \tau[\rho_{1p}(\mathbf{r}) + \rho_{1n}(\mathbf{r})] \\ & - \tau[\rho_{2p}(\mathbf{r}) + \rho_{2n}(\mathbf{r})] \} d\mathbf{r}, \end{aligned} \quad (20)$$

where τ denotes the kinetic-energy density. Two nuclei are overlapping at R and completely separated at infinity, $R = \infty$. Such modifications improve the consistency between calculated α decay half-lives and experimental data [43]. In this study, we applied the same modification to the DF model. Therefore, the total interaction potential (1) changes to

$$V(R) = V_C(R) + \lambda[V_N(R) + \Delta K(R)]. \quad (21)$$

Typically, the effects of applying different density distributions calculated by SLy4 and OMGA on the total potential calculations for the nucleus ^{294}Og are shown in Fig. 2. The presented results in this figure indicate that the application of different density distributions can cause a sensible variation at the inner part of the total potential, especially from the region with complete overlap to the distance of about 13 fm. As shown in this figure, the second turning point R_2 is changed by the different total potential calculated by SLy4 and OMGA, and the first and third turning points are unchanged. The different interaction potential obtained by the SLy4 and OMGA forces would be due to the different nuclear matter properties associated with these forces, illustrated in Table II, causing characteristic situations in the dinuclear system. Therefore, the α decay properties would be impacted by applying different density distributions [43,62].

As mentioned above, one of the mechanisms that have been extensively used to adjust NN interactions, applying the clusterization state in the dinuclear system and reproducing α decay energy in the total system, is the renormalization of the strength of effective NN interactions due to the BS quantization condition. This mechanism provides an opportunity for systematic investigations of nuclear properties in α decay chains [1].

In the first step, the α decay chains $^{296}\text{118} \rightarrow ^{284}\text{Cn}$ and $^{298}\text{120} \rightarrow ^{282}\text{Cn}$ are considered. To calculate the interaction potential, the DF model based on the effective M3Y nucleon-

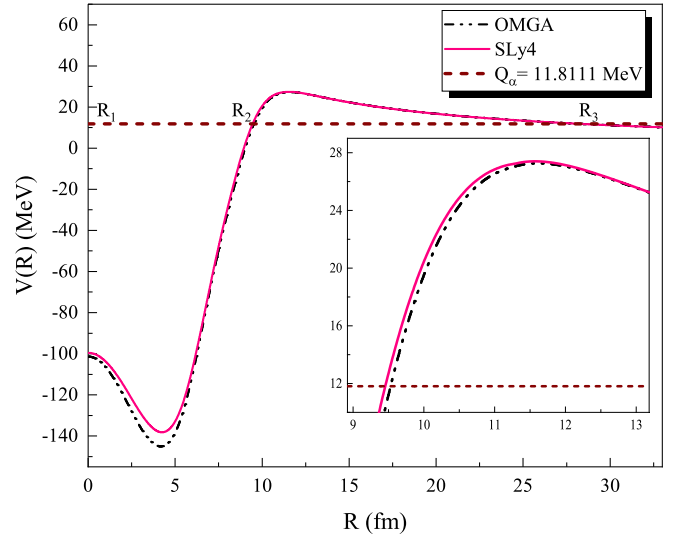


FIG. 2. Calculated total potentials within different nucleon density distributions corresponding to the SLy4 and OMGA Skyrme forces, typically for the nucleus ^{294}Og . The classical turning points are presented schematically. For $0^+ \rightarrow 0^+s$ -wave decay the inner turning point is at $R_1 = 0$.

nucleon interaction is adopted in which the nucleon density distributions are being determined by the self-consistent HFB calculations based on the set of Skyrme SLy4 and OMGA parametrization.

The potential strength parameter λ is adjusted to the energy of the alpha particle in α emitters $(A + 4) = A \otimes \alpha$. The λ parameters corresponding to SLy4 and OMGA for the considered chains $^{296}\text{118} \rightarrow ^{284}\text{Cn}$ and $^{298}\text{120} \rightarrow ^{282}\text{Cn}$ are presented in Fig. 3(a) with respect to the atomic number of the parent nuclei. The expressed differences between λ parameters obtained from SLy4 and OMGA presented in Fig. 3 can be due to the different isospin asymmetries and intrinsic nuclear matter properties complemented in SLy4 and OMGA, which are proceeding to the various nucleon density distributions [78–81]. Therefore, one would expect that the interaction potentials obtained by the density-dependent DF model would be affected.

The obtained strength parameters λ are leading to volume integrals J_R per the interacting nucleon pair around 300 MeV fm^3 , which is expressed by

$$J_R = -\frac{4\pi}{A_\alpha A_d} \int_0^\infty V_N(R) R^2 dR. \quad (22)$$

Note that, as usual, the negative sign of J_R is omitted in this work. The corresponded volume integrals J_R to the SLy4 and OMGA for the desired chains $^{296}\text{118} \rightarrow ^{284}\text{Cn}$ and $^{298}\text{120} \rightarrow ^{282}\text{Cn}$ are presented in Fig. 3(b). As shown in Fig. 3, by adopting the almost equal slope reduction in the treatment of λ parameters and the smooth and gradual reductions of 2 MeV fm^3 units from one α emitter to another in the obtained volume integrals, one might hope to obtain reliable extrapolate volume integrals, λ parameters, and then Q values of the unknown nuclei $^{296}\text{118}$ and $^{298}\text{120}$. As shown in Fig. 3(b), the equal slope reduction of volume integrals for

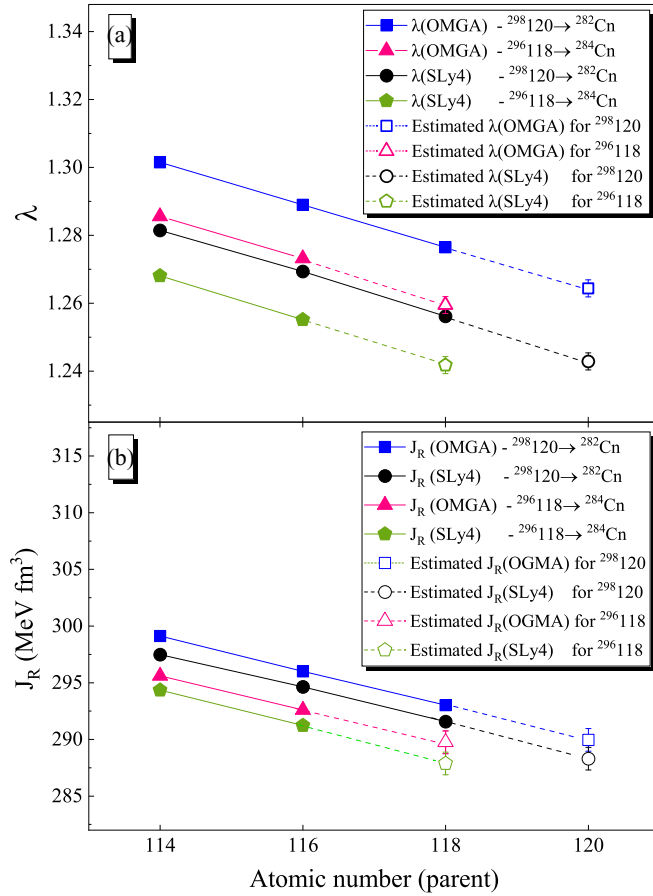


FIG. 3. (a) Values of the λ parameters for decay chains $^{296}\text{118} \rightarrow ^{284}\text{Cn}$ and $^{298}\text{120} \rightarrow ^{282}\text{Cn}$. (b) Volume integrals for these decay chains.

SLy4 and OMGA forces lead to the same uncertainty for the λ -parameter predictions of the unknown nuclei $^{296}\text{118}$ and $^{298}\text{120}$, which is about 0.001. The λ parameters corresponding to SLy4 and OMGA extrapolated for $^{296}\text{118}$ within the obtained volume integrals are about 1.2418 ± 0.001 and 1.2595 ± 0.001 , respectively.

Also, the α decay energy for unknown $^{296}\text{118}$ can be estimated through the BS condition and the resulting volume integrals J_R and λ values of the nuclear potentials corresponding to the SLy4 and OMGA Skyrme forces. The resulting Q values for $^{296}\text{118}$ are 11.3727 ± 0.0030 and 11.7109 ± 0.0030 MeV for SLy4 and OMGA, respectively. For comparison, 11.726 MeV was reported for the Q_α value of $^{296}\text{118}$ within the WS4 + RBF model [24]. The Q_α value of $^{296}\text{118}$ obtained within OMGA is very close to the estimation of the WS4 + RBF model.

Moreover, the estimated half-lives for $^{296}\text{118}$ range from 1.60 to 0.02 ms for SLy4 and OMGA, respectively. It is noticeable that these α decay half-lives are calculated with the $P_\alpha = 1$ assumption. Extensively, it has been shown that the alpha formation probability has a remarkable role in α decay studies [82–84]. Due to the fact that most SHN are α emitters, the preformation probabilities that are estimated from the CFM are adopted to apply the clusterization states

to the total system, which are expressed as P_α^{CFM} in Table III. Consequently, for applying clusterization states to the calculations, the average preformation probabilities in the decay chain are used for $^{296}\text{118}$. Therefore, the affected half-lives for $^{296}\text{118}$ from clusterization states, $P_\alpha^{\text{CFM}} = 0.18$, change to 8.88 and 0.15 ms for SLy4 and OMGA, which are of the order of the prediction models WS3⁺, WS4 + RBF, and HN. The calculated half-lives corresponding to SLy4 and OMGA are presented as $T_{1/2}^{\text{SLy4}}$ and $T_{1/2}^{\text{OMGA}}$ in Table III.

Furthermore, the systematic behavior of α decay parameters for α decay chains $^{298}\text{120} \rightarrow ^{282}\text{Cn}$ is investigated. To predict nuclear properties of the unknown nucleus $^{298}\text{120}$, the volume integrals and λ parameters of the decay chain $^{298}\text{120} \rightarrow ^{282}\text{Cn}$ are also being analyzed. The obtained results are presented in Fig. 3. As illustrated in Fig. 3(b), the estimated volume integrals of $^{298}\text{120}$ are 288.302 ± 2 and 289.958 ± 2 MeV fm^3 that are associated with the λ parameters 1.2429 ± 0.001 and 1.2644 ± 0.001 for SLy4 and OMGA, respectively. Consequently, the Q values 11.9415 ± 0.0030 and 12.0454 ± 0.0030 MeV are estimated through the λ parameters and BS condition corresponding to SLy4 and OMGA. For comparison, the Q_α value estimated by OMGA is closer to the WS4 + RBF model, $Q = 11.981$ MeV, for the unknown nucleus $^{298}\text{120}$. Consequently, the preformation probability $P_\alpha^{\text{CFM}} = 0.18$ is estimated by the CFM for the unknown nucleus $^{298}\text{120}$. Therefore, the impacted half-lives from the clustering effects of $^{298}\text{120}$ are also 0.22 and 0.098 ms belonging to SLy4 and OMGA.

As illustrated results in Fig. 3, the λ parameters and volume integrals of two neighbor chains are expressing the same decreasing treatment with equal slope. However, this tendency can create an opportunity that extrapolation on the specific decay chain is being fulfilled. Hence the α decay chains $^{274}\text{112} \rightarrow ^{214}\text{Pb}$ and $^{268}\text{110} \rightarrow ^{212}\text{Pb}$ are being considered in the second step.

Consequently, the obtained λ parameters for $^{274}\text{112}$ and $^{268}\text{110}$ are presented in Fig. 4. As shown in this figure, the λ parameters have a same decreasing tendency with equal slope according to the fact that the two α decay chains $^{274}\text{112} \rightarrow ^{214}\text{Pb}$ and $^{268}\text{110} \rightarrow ^{212}\text{Pb}$ are adjacent. As shown in Figs. 4(a) and 4(b), the volume integrals 293.517 ± 2 and 294.017 ± 2 MeV fm^3 are being extrapolated for $^{274}\text{112}$, which proceeds to the λ parameters 1.2652 ± 0.001 and 1.2790 ± 0.001 by use of SLy4 and OMGA, respectively.

The extrapolated λ parameters for the unknown nucleus $^{274}\text{112}$ are proceeding to the Q values 12.1755 ± 0.0030 and 11.8108 ± 0.0030 MeV, corresponding to SLy4 and OMGA, respectively. For the nucleus $^{274}\text{112}$, $Q = 11.520$ MeV is also reported by the WS4 + RBF model. Furthermore, the estimated alpha preformation probability $P_\alpha^{\text{CFM}} = 0.16$ is calculated by the CFM for $^{274}\text{112}$. Therefore, the α decay half-lives are 0.59 and 2.91 μs and can be expected for $^{274}\text{112}$ corresponding to SLy4 and OMGA, respectively.

In addition, λ parameters and volume integrals of the α decay chain $^{268}\text{110} \rightarrow ^{212}\text{Pb}$ are also examined, which are presented in Figs. 4 and 5. The volume integrals 293.430 ± 2 and 294.529 ± 2 MeV fm^3 are extrapolated for $^{268}\text{110}$, which proceeding to λ parameters 1.2655 ± 0.001 and $1.2808 \pm$

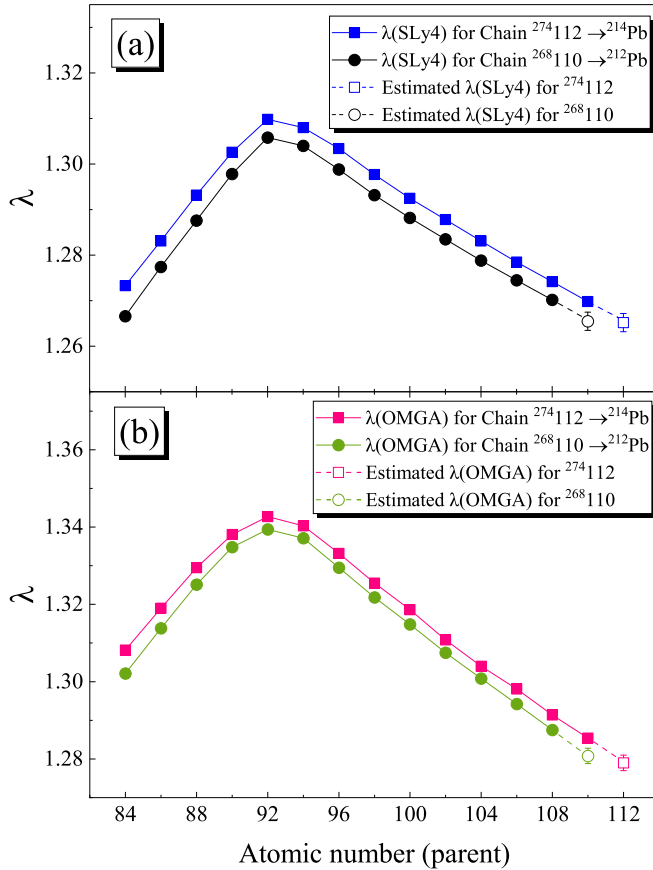


FIG. 4. (a) Values of the λ parameters for decay chains $^{274}112 \rightarrow ^{214}\text{Pb}$ and $^{268}110 \rightarrow ^{212}\text{Pb}$ from SLy4 force. (b) Corresponding λ parameters for mentioned decay chains obtained by OMGA force.

0.001 by use of SLy4 and OMGA, respectively. Consequently, the Q values 11.4830 ± 0.0030 and 11.5826 ± 0.0030 MeV corresponding to SLy4 and OMGA can be expected by employing the BS condition. Through applying the alpha-formation probability $P_{\alpha}^{\text{CFM}} = 0.18$ obtained for $^{268}110$, the half-lives 4.60 and 2.47 μs for $^{268}110$ corresponding to the SLy4 and OMGA forces are estimated by considering the obtained Q values, respectively.

IV. SUMMARY AND CONCLUSION

Ground-state properties of nuclei, such as rms radii and binding energies, can be reproduced fairly well by using mean-field models with effective interactions such as the Skyrme interactions. In this study, the α decay properties of unknown SHN were explored. To this end, the systematic behavior of parameters of α -nucleus DF potentials was considered. Consequently, the α core potentials are calculated by the DF model associated with the density distributions of the protons, and neutrons were calculated using the

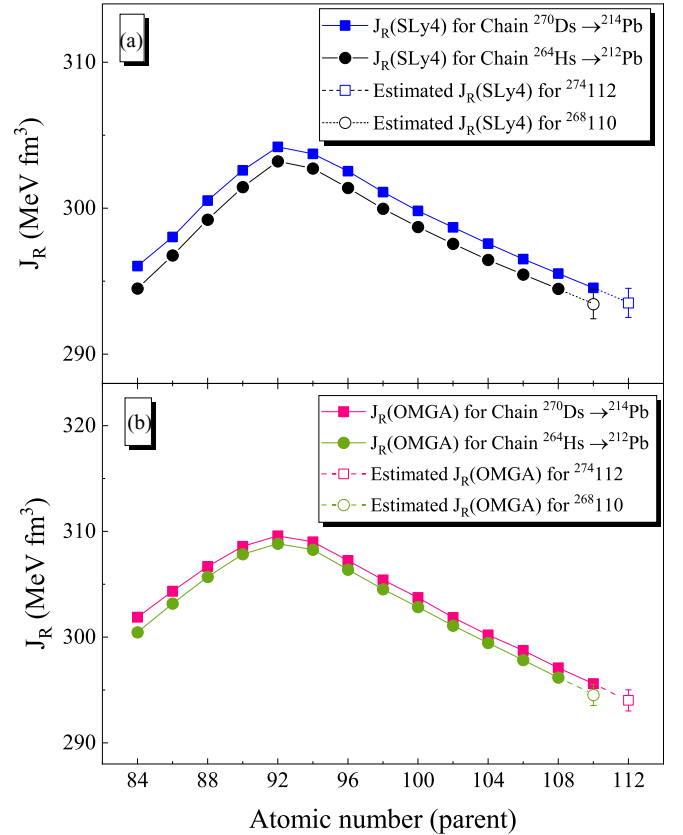


FIG. 5. (a) Values of the volume integrals for decay chains $^{274}112 \rightarrow ^{214}\text{Pb}$ and $^{268}110 \rightarrow ^{212}\text{Pb}$ from SLy4 force. (b) Corresponding volume integrals for mentioned decay chains obtained by OMGA force.

self-consistent HFB calculations based on SLy4. Also, the OMGA mean field was optimized to account for well-reproducing ground-state properties of the SHN with $82 \leq Z \leq 120$. In turn, the density distributions calculating by this optimized mean-field are adopted to verify α decay properties of unknown SHN. The obtained results through the OMGA force indicated that the nuclear properties of SHN are more consistent with experimental data and the WS4 + RBF mass model exposing that the theoretical studies on α decay properties would be affected by the choice of Skyrme interaction. Hopefully, more precise anticipations can be expected by choosing an appropriate mean field describing the nuclear properties of SHN.

ACKNOWLEDGMENTS

The authors gratefully thank Dr. Peter Mohr for his valuable comments and many encouraging discussions on the α -nucleus potentials and DF model.

[1] P. Mohr, *Phys. Rev. C* **95**, 011302 (2017).

[2] N. Wang, M. Liu, Xizhen Wu, and J. Meng, *Phys. Rev. C* **93**, 014302 (2016).

[3] A. Sobczewski, *Phys. Rev. C* **94**, 051302(R) (2016).

[4] K. Anjali, K. Prathapan, and R. Biju, *Nucl. Phys. A* **993**, 121644 (2020).

- [5] N. A. Alsaif and S. M. S. Ahmed, *Results Phys.* **12**, 1158 (2019).
- [6] A. I. Budaca, R. Budaca, and I. Silisteanu, *Nucl. Phys. A* **951**, 60 (2016).
- [7] J. M. Dong, W. Zuo, J. Z. Gu, Y. Z. Wang, and B. B. Peng, *Phys. Rev. C* **81**, 064309 (2010).
- [8] F. Li, L. Zhu, Z.-H. Wu, X.-B. Yu, J. Su, and C.-C. Guo, *Phys. Rev. C* **98**, 014618 (2018).
- [9] P. Mohr, Zs. Fülöp, Gy. Gyürky, G. G. Kiss, and T. Szücs, *Phys. Rev. Lett.* **124**, 252701 (2020).
- [10] Y. T. Oganessian *et al.*, *Phys. Rev. C* **79**, 024603 (2009).
- [11] G. L. Zhang, X. Y. Le, and H. Q. Zhang, *Phys. Rev. C* **80**, 064325 (2009).
- [12] X. J. Bao, Y. Gao, J. Q. Li, and H. F. Zhang, *Phys. Rev. C* **91**, 011603 (2015).
- [13] X. J. Bao, S. Q. Guo, H. F. Zhang, Y. Z. Xing, J. M. Dong, and J. Q. Li, *J. Phys. G* **42**, 085101 (2015).
- [14] J. P. Cui, Y. L. Zhang, S. Zhang, and Y. Z. Wang, *Phys. Rev. C* **97**, 014316 (2018).
- [15] O. N. Ghodsi and M. Hassanzad, *Phys. Rev. C* **101**, 034606 (2020).
- [16] P. A. Ellison *et al.*, *Phys. Rev. Lett.* **105**, 182701 (2010).
- [17] Y. Oganessian and V. Utyonkov, *Nucl. Phys. A* **944**, 62 (2015).
- [18] Y. T. Oganessian *et al.*, *Phys. Rev. C* **83**, 054315 (2011).
- [19] J. M. Gates *et al.*, *Phys. Rev. Lett.* **121**, 222501 (2018).
- [20] K. E. Gregorich *et al.*, *Phys. Rev. C* **72**, 014605 (2005).
- [21] Y. Oganessian, *J. Phys. G* **34**, R165 (2007).
- [22] N. G. Kelkar and M. Nowakowski, *J. Phys. G* **43**, 105102 (2016).
- [23] N. Wang and M. Liu, *Phys. Rev. C* **84**, 051303(R) (2011).
- [24] N. Wang, M. Liu, X. Wu, and J. Meng, *Phys. Lett. B* **734**, 215 (2014).
- [25] I. Muntian, Z. Patyk, and A. Sobiczewski, *Acta Phys. Pol. B* **32**, 691 (2001).
- [26] M. Ismail, W. M. Seif, A. Adel, and A. Abdurrahman, *Nucl. Phys. A* **958**, 202 (2017).
- [27] P. Mohr, *Phys. Rev. C* **73**, 031301(R) (2006); **74**, 069902(E) (2006).
- [28] M. Samyn *et al.*, *Nucl. Phys. A* **700**, 142 (2002).
- [29] B. A. Brown, G. Shen, G. C. Hillhouse, J. Meng, and A. Trzcińska, *Phys. Rev. C* **76**, 034305 (2007).
- [30] E. Chabanat, P. Bonche, P. Haensel, J. Meyer, and R. Schaeffer, *Nucl. Phys. A* **635**, 231 (1998).
- [31] J. Friedrich and P.-G. Reinhard, *Phys. Rev. C* **33**, 335 (1986).
- [32] J. C. Pei, F. R. Xu, Z. J. Lin, and E. G. Zhao, *Phys. Rev. C* **76**, 044326 (2007).
- [33] J. C. Pei, F. R. Xu, and P. D. Stevenson, *Phys. Rev. C* **71**, 034302 (2005).
- [34] R. K. Gupta, D. Singh, R. Kumar, and W. Greiner, *J. Phys. G* **36**, 075104 (2009).
- [35] M. Centelles, X. Roca-Maza, X. Viñas, and M. Warda, *Phys. Rev. C* **82**, 054314 (2010).
- [36] G. R. Satchler and W. G. Love, *Phys. Rep.* **55**, 183 (1979).
- [37] A. M. Kobos, B. A. Brown, R. Lindsay, and G. R. Satchler, *Nucl. Phys. A* **425**, 205 (1984).
- [38] D. T. Khoa and W. von Oertzen, *Phys. Lett. B* **304**, 8 (1993).
- [39] D. N. Basu, *J. Phys. G* **29**, 2079 (2003).
- [40] K. Bennaceur and J. Dobaczewski, *Comput. Phys. Commun.* **168**, 96 (2005).
- [41] S. Ćwiok, W. Nazarewicz, and P. H. Heenen, *Phys. Rev. Lett.* **83**, 1108 (1999).
- [42] A. Mukherjee, D. J. Hinde, M. Dasgupta, K. Hagino, J. O. Newton, and R. D. Butt, *Phys. Rev. C* **75**, 044608 (2007).
- [43] M. Moghaddari Amiri and O. N. Ghodsi, *Phys. Rev. C* **102**, 054602 (2020).
- [44] B. Cai, G. Chen, J. Xu, C. Yuan, C. Qi, and Y. Yao, *Phys. Rev. C* **101**, 054304 (2020).
- [45] W. M. Seif and A. Adel, *Phys. Rev. C* **99**, 044311 (2019).
- [46] P. Mohr, *Phys. Rev. C* **61**, 045802 (2000).
- [47] M. Ismail and A. Adel, *J. Phys. G* **44**, 125106 (2017).
- [48] B. Buck, A. C. Merchant, and S. M. Perez, *At. Data Nucl. Data Tables* **54**, 53 (1993).
- [49] B. Buck, A. C. Merchant, and S. M. Perez, *At. Data Nucl. Data Tables* **51**, 559 (1995).
- [50] B. Buck, J. C. Johnston, A. C. Merchant, and S. M. Perez, *Phys. Rev. C* **53**, 2841 (1996).
- [51] K. Wildermuth and Y. Tang, *A Unified Theory of the Nucleus* (Vieweg, Braunschweig, 1977).
- [52] S. A. Gurrvitz and G. Kälbermann, *Phys. Rev. Lett.* **59**, 262 (1987).
- [53] T. L. Zhao and X. J. Bao, *Phys. Rev. C* **98**, 064307 (2018).
- [54] S. M. S. Ahmed, R. Yahaya, S. Radiman, and M. S. Yasir, *J. Phys. G* **40**, 065105 (2013).
- [55] J. G. Deng, J. C. Zhao, P. C. Chu, and X. H. Li, *Phys. Rev. C* **97**, 044322 (2018).
- [56] D. Deng, Z. Ren, D. Ni, and Y. Qian, *J. Phys. G* **42**, 075106 (2015).
- [57] K. Varga, R. G. Lovas, and R. J. Liotta, *Phys. Rev. Lett.* **69**, 37 (1992).
- [58] K. Varga, R. G. Lovas, and R. Liotta, *Nucl. Phys. A* **550**, 421 (1992).
- [59] S. Goriely, S. Hilaire, M. Girod, and S. Péru, *Phys. Rev. Lett.* **102**, 242501 (2009).
- [60] P. Ring, *Prog. Part. Nucl. Phys.* **37**, 193 (1996).
- [61] G. A. Lalazissis, J. König, and P. Ring, *Phys. Rev. C* **55**, 540 (1997).
- [62] M. M. Amiri and O. N. Ghodsi, *Chin. Phys. C* **44**, 054107 (2020).
- [63] W. Ryssens, V. Hellemans, M. Bender, and P.-H. Heenen, *Comput. Phys. Commun.* **187**, 175 (2015).
- [64] D. Ni and Z. Ren, *Phys. Rev. C* **92**, 054322 (2015).
- [65] A. Trzcińska, J. Jastrzebski, P. Lubinski, F. J. Hartmann, R. Schmidt, T. von Egidy, and B. Klos, *Phys. Rev. Lett.* **87**, 082501 (2001).
- [66] B. Avez, C. Simenel, and P. Chomaz, *Phys. Rev. C* **78**, 044318 (2008).
- [67] L. Zurek, E. A. Coello Pérez, S. K. Bogner, R. J. Furnstahl, and A. Schwenk, *Phys. Rev. C* **103**, 014325 (2021).
- [68] Di Wu, C. L. Bai, H. Sagawa, and H. Q. Zhang, *Phys. Rev. C* **102**, 054323 (2020).
- [69] W. M. Seif, *Phys. Rev. C* **74**, 034302 (2006).
- [70] I. Angeli and K. Marinova, *At. Data Nucl. Data Tables* **99**, 69 (2013).
- [71] D. Ni, Z. Ren, T. Dong, and Y. Qian, *Phys. Rev. C* **87**, 024310 (2013).
- [72] X. Xia, Y. Lim, P. Zhao, H. Liang, X. Qu, Y. Chen, H. Liu, L. Zhang, S. Zhang, Y. Kim, and J. Meng, *At. Data Nucl. Data Tables* **121–122**, 1 (2018).
- [73] K. Cheng and C. Xu, *Phys. Rev. C* **99**, 014607 (2019).

- [74] W. Seif, A. Abdelhady, and A. Adel, *J. Phys. G* **45**, 115101 (2018).
- [75] H. Esbensen and Ş. Mişicu, *Phys. Rev. C* **76**, 054609 (2007).
- [76] D. Vautherin and D. M. Brink, *Phys. Rev. C* **5**, 626 (1972).
- [77] F. L. Stancu and D. M. Brink, *Nucl. Phys. A* **270**, 236 (1976).
- [78] M. Dutra, O. Lourenco, J. S. SaMartins, A. Delfino, J. R. Stone, and P. D. Stevenson, *Phys. Rev. C* **85**, 035201 (2012).
- [79] W. M. Seif, M. Shalaby, and M. F. Alrakshy, *Phys. Rev. C* **84**, 064608 (2011).
- [80] E. Shin, Y. Lim, Chang Ho Hyun, and Y. Oh, *Phys. Rev. C* **94**, 024320 (2016).
- [81] B. Gheshlagh and O. Ghodsi, *Chin. Phys. C* **43**, 124105 (2019).
- [82] M. Ismail and A. Adel, *Phys. Rev. C* **86**, 014616 (2012).
- [83] W. M. Seif, M. Ismail, and E. T. Zeini, *J. Phys. G* **44**, 055102 (2017).
- [84] H. F. Zhang, J. M. Dong, G. Royer, W. Zuo, and J. Q. Li, *Phys. Rev. C* **80**, 037307 (2009).